

RELATIVISTIC RING MODELS

MAXIMILIANO UJEVIC

*Centro de Ciências Naturais e Humanas, Universidade Federal do ABC, 09210-170
Santo André, São Paulo, Brasil
mujevic@ufabc.edu.br*

PATRICIO S. LETELIER

*Departamento de Matemática Aplicada, Instituto de Matemática, Estatística e Computação
Científica, Universidade Estadual de Campinas, 13081-970
Campinas, São Paulo, Brasil
letelier@ime.unicamp.br*

DANIEL VOGT

*Departamento de Matemática Aplicada, Instituto de Matemática, Estatística e Computação
Científica, Universidade Estadual de Campinas, 13081-970
Campinas, São Paulo, Brasil
dvogt@ime.unicamp.br*

Dedicated to the memory of Professor Patricio S. Letelier

Relativistic thick ring models are constructed using previously found analytical Newtonian potential-density pairs for flat rings and toroidal structures obtained from Kuzmin-Toomre family of discs. In particular, we present systems with one ring, two rings and a disc with a ring. Also, the circular velocity of a test particle and its stability when performing circular orbits are presented in all these models. In general, we find that regions of non-stability appear between the rings when they become thinner.

Keywords: Keyword1; keyword2; keyword3.

1. Introduction

Ring structures are common features in different astrophysical objects on different scales. In particular, we have ring structures in the giant planets of the Solar system and also in several ring galaxies (or R galaxies) which are objects with approximate elliptical rings and no luminous matter visible in their interiors.^{1,2} Furthermore, sometimes, as the result of interactions between galaxies, a ring of gas and stars is formed and rotates over the poles of a galaxy, resulting in the polar-ring galaxies.³ In Newtonian gravity, the potential of a ring enclosing a disc can be obtained by a process of complexification of the potential of a punctual mass.^{4,5,6} This potential was used to build a family of similar structures.⁷ Also, the Lord Kelvin inversion theorem⁸ can be used to invert a member of the Morgan & Morgan family of discs⁹ to produce an infinite disc with a central hole of the same radius as

the original disc. We can define a cut-off in these inverted disc to represent flat rings. Furthermore, Letelier constructed several families of flat rings using the superposition of Morgan and Morgan discs of different densities.¹⁰ Recently, Vogt & Letelier¹¹ found potential-density pairs representing flat ring structures by superposing members of the classical Kuzmin-Toomre family of discs.^{12,13} By using a suitable transformation, they found that these flat ring systems can be used to generate three dimensional potential-density pairs with toroidal mass distribution. The main advantage of these toroidal mass distribution models is that the density and the gravitational potential are given in terms of elementary functions. Also, similar toroidal analytical systems have been obtained using a different technique, known as the complex-shift method.^{14,15} In general relativity, the properties of space-times that represent superpositions of a Schwarzschild black hole and a disc or ring were investigated by several authors.^{16,17,18,19} The purpose of this article is to consider three-dimensional models for the gravitational field of rings and disc with rings in the context of general relativity following the method used in Ref. 20. As a very first test for stability, we study the stability of particles in circular orbits using the relativistic version²¹ of the Rayleigh criterion of stability.^{22,23} We know that a better approach to study its stability is by performing first order perturbations of the energy-momentum tensor that take into account the collective behavior of the particles.^{24,25,26} This study will be done in a future work.

The article is organized as follows. In Section 2, we present a special form of the isotropic Schwarzschild metric and the components of the energy-momentum tensor as functions of the metric coefficients, from which the physical properties of the matter distribution can be calculated. We also write expressions for the tangential circular velocity and specific angular momentum of test particles in circular motion. In Section 3, we apply the results of Section 2 to a single ring system, a disc with a ring system and a double ring system, which are particular cases of a family of solution found in Ref. 11. Finally, in Section 4, we summarize our results.

2. Einstein Equations

In General Relativity are two methods to find exact solutions of Einstein's field equations. The first method is the so called direct method, in which we set the energy-momentum tensor and then we find the metric tensor. In the other hand, most of the models (for example, disks and rings in astrophysics) were found by using the inverse method, in which we use the metric to calculate its energy-momentum tensor. In this article we used the second. But, not every solution found using this method is physical acceptable. The models must satisfy the energy criteria and also is desirable to have a clear physical interpretation at the newtonian limit. So, the justification of the method is done a posteriori and it will depend of the outcome. With this in consideration, let us consider the particular case of axially symmetric

spacetimes in isotropic coordinates

$$ds^2 = \left(\frac{1-f}{1+f} \right)^2 c^2 dt^2 - (1+f)^4 (dR^2 + dz^2 + R^2 d\varphi^2), \quad (1)$$

where R , φ and z are the usual cylindrical coordinates and $f = f(R, z)$. From Einstein equations, $G_{\mu\nu} = -(8\pi G/c^4)T_{\mu\nu}$, and the metric (1) we obtain the following expressions for the components of the energy-momentum tensor

$$T_t^t = -\frac{c^4}{2\pi G(1+f)^5} \left(f_{,RR} + f_{,zz} + \frac{f_{,R}}{R} \right), \quad (2)$$

$$T_R^R = \frac{c^4}{4\pi G(1+f)^5(1-f)} \left(ff_{,zz} + \frac{ff_{,R}}{R} + 2f_{,R}^2 - f_{,z}^2 \right), \quad (3)$$

$$T_z^z = \frac{c^4}{4\pi G(1+f)^5(1-f)} \left(ff_{,RR} + \frac{ff_{,R}}{R} + 2f_{,z}^2 - f_{,R}^2 \right), \quad (4)$$

$$T_\varphi^\varphi = \frac{c^4}{4\pi G(1+f)^5(1-f)} [f(f_{,RR} + f_{,zz}) - f_{,R}^2 - f_{,z}^2], \quad (5)$$

$$T_z^R = T_R^z = -\frac{c^4}{4\pi G(1+f)^5(1-f)} (ff_{,Rz} - 3f_{,R}f_{,z}). \quad (6)$$

In the Newtonian limit, i.e. when $f \ll 1$, equation (2) reduces to the Poisson equation if the function f is related to the Newtonian gravitational potential Φ by $g_{00} = 1 + 2\Phi/c^2$, which means that

$$f = -\Phi/2c^2. \quad (7)$$

Note that it is a desirable property for every metric to obtain a physical consistent newtonian limit, and always we interpret the four dimensional metric based on this limit. As an example, we interpret the exterior Schwarzschild solution as the space-time solution of a spherical symmetric mass body because in its newtonian limit we obtain the gravitational potential of a point mass. If the solution does not have a consistent newtonian limit then it is, in some sense, useless. If we use a potential of the form $\Phi = A/\sqrt{R^2 + z^2}$ in (7), where A is a constant, then we obtain the vacuum solution.

To find the energy density ρ and the stresses (pressures or tensions) of the fluid we must solve the eigenvalue problem for the energy-momentum tensor $T_\beta^\alpha V^\beta = \lambda V^\alpha$. In this way, we can write the energy-momentum tensor in diagonal form

$$T^{\alpha\beta} = \rho e_{(0)}^\alpha e_{(0)}^\beta + p_+ e_{(1)}^\alpha e_{(1)}^\beta + p_- e_{(2)}^\alpha e_{(2)}^\beta + p_\varphi e_{(3)}^\alpha e_{(3)}^\beta, \quad (8)$$

where

$$\rho = \frac{T_t^t}{c^2}, \quad p_\pm = -\frac{T_R^R + T_z^z}{2} \mp \frac{1}{2} \sqrt{(T_R^R - T_z^z)^2 + 4(T_z^R)^2}, \quad p_\varphi = -T_\varphi^\varphi, \quad (9)$$

and

$$e_{(0)}^\alpha = \left(\frac{1+f}{1-f}, 0, 0, 0 \right), \quad e_{(1)}^\alpha = \left(0, e_{(1)}^R, e_{(1)}^z, 0 \right), \quad (10)$$

$$e_{(2)}^\alpha = \left(0, e_{(2)}^R, e_{(2)}^z, 0 \right), \quad e_{(3)}^\alpha = \left(0, 0, 0, \frac{1}{R(1+f)^2} \right), \quad (11)$$

4 *M. Ujevic, P. S. Letelier and D. Vogt*

where

$$e_{(1)}^R = -\frac{T_z^R}{(1+f)^2 \sqrt{(T_z^R)^2 + (T_R^R + p_+)^2}}, \quad (12)$$

$$e_{(1)}^z = \frac{T_R^R + p_+}{(1+f)^2 \sqrt{(T_z^R)^2 + (T_R^R + p_+)^2}}, \quad (13)$$

$$e_{(2)}^R = -\frac{T_z^R}{(1+f)^2 \sqrt{(T_z^R)^2 + (T_R^R + p_-)^2}}, \quad (14)$$

$$e_{(2)}^z = \frac{T_R^R + p_-}{(1+f)^2 \sqrt{(T_z^R)^2 + (T_R^R + p_-)^2}}. \quad (15)$$

In this case the Newtonian effective density is written as $\epsilon = \rho + p_-/c^2 + p_+/c^2 + p_\varphi/c^2 = \rho - T_R^R/c^2 - T_z^z/c^2 - T_\varphi^\varphi/c^2$. The strong energy condition requires that $\epsilon \geq 0$, whereas the weak energy condition imposes the condition $\rho \geq 0$. The dominant energy condition requires that $|p_R/\rho| \leq c^2$, $|p_z/\rho| \leq c^2$ and $|p_\varphi/\rho| \leq c^2$.

Assuming circular geodesic motion of a particle in the equatorial plane of the model, we can obtain two interesting physical quantities, i.e. the tangential velocity v_c , often known as the rotation profile, and the angular momentum h . This quantities can be written as²⁷

$$v_c^2 = -\frac{2c^2 R f_{,R}}{(1-f)(1+f+2Rf_{,R})}, \quad (16)$$

$$h = cR^2(1+f)^2 \sqrt{\frac{-2f_{,R}}{R[1-f^2+2Rf_{,R}(2-f)]}}, \quad (17)$$

and must be evaluated in $z = 0$. The angular momentum written above, can be used as an stability criterion for circular orbits on the galactic plane by using an extension of the Rayleigh criterion of stability of a fluid at rest in a gravitational field^{22,23}

$$h \left. \frac{dh}{dR} \right|_{z=0} > 0. \quad (18)$$

3. Ring models

In a recent work, Vogt & Letelier¹¹ presented families of flat rings that were constructed by superposing members of the Kuzmin-Toomre family of discs. In particular they found a family for single flat rings, double flat rings and discs with flat rings. One way to generate three-dimensional potential-density from flat ring models is to inflate the rings performing the transformation $|z| \rightarrow \sqrt{z^2 + b^2}$. This is the same transformation used by Miyamoto & Nagai²⁸ to inflate the Kuzmin-Toomre discs. In the next subsections we construct general relativistic thick models of rings based on these flat rings families.

3.1. Single ring system

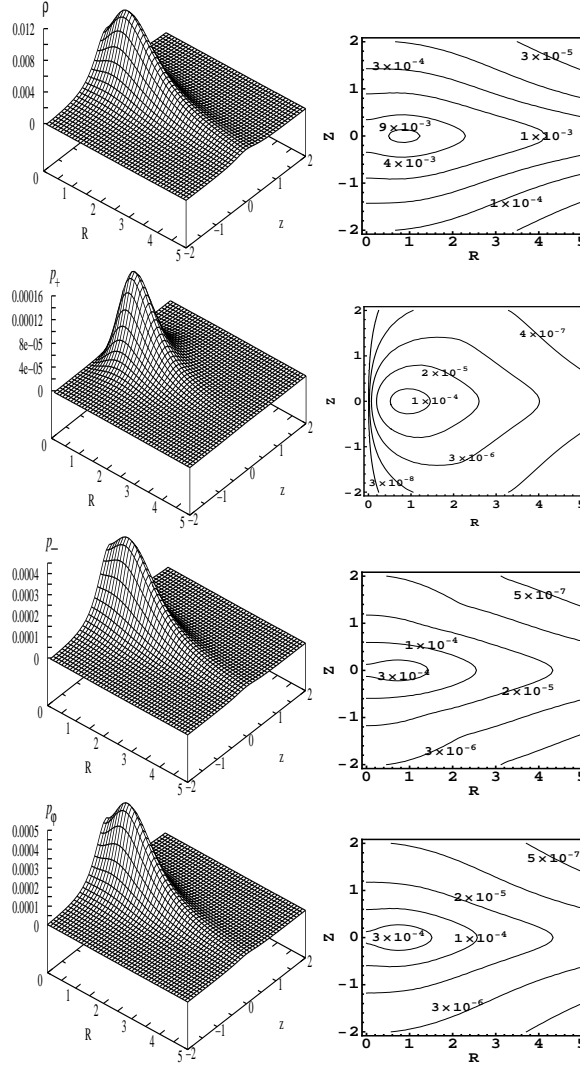


Fig. 1. Surface plots and level curves for the energy density and the stresses for the case of a general relativistic version of the single ring. The parameter values are $a = 1$, $b = 0.5$ and $\sigma_c = 0.1$.

For a general relativistic ring system, we start by taking the first member of the family of a single flat ring, which is

$$\phi = -\frac{2\pi\sigma_c G a^2}{3[R^2 + (a + |z|)^2]^{3/2}}(2R^2 + 2|z|^2 + a^2 + 3a|z|), \quad (19)$$

where a is a constant related to the Kuzmin-Toomre potential, G is Newton's grav-

6 *M. Ujevic, P. S. Letelier and D. Vogt*

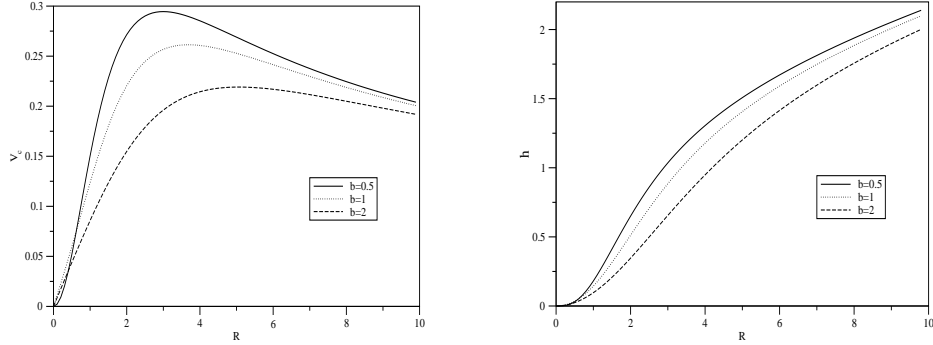


Fig. 2. Tangential velocity and angular momentum for a particle orbiting the $z = 0$ plane for the same parameter values of Fig. 1 and $b = 0.5, 1, 2$. The criterion of stability indicates that all the orbits depicted are stable.

itational constant, σ_c is a constant with dimension of surface density and (R, z) are the usual cylindrical coordinates. In Ref. 11 notation, this potential corresponds to $\phi^{(1,0)}$, which is the first member of the flat single ring potential of Appendix B in the cited article. To generate the three dimensional ring model we perform the transformation $|z| \rightarrow \sqrt{z^2 + b^2}$ and we obtain

$$\Phi = -\frac{2\pi\sigma_c G a^2}{3\chi^{3/2}}(2R^2 + 2\xi^2 + a^2 + 3a\xi). \quad (20)$$

where $\xi = \sqrt{z^2 + b^2}$ and $\chi = R^2 + (a + \xi)^2$. Note that in the above equation we change the notation from ϕ to Φ . Now, from equation (7) we obtain the function f and then we can find the energy density, ρ , and the stresses (pressures or tensions),

p_- , p_+ , p_φ , using the relations (2)-(6), say

$$T_t^t = \frac{a^2 b^2 c^2 \sigma_c}{2\xi^3 \chi^{7/2} (1+f)^5} [2\xi^3 (R^2 + \xi^2) + a^3 (R^2 + 2\xi^2) + a^2 \xi (7R^2 + 6\xi^2) + a(R^4 + 8\xi^2 R^2 + 6\xi^4)], \quad (21)$$

$$T_R^R = -\frac{a^4 G \pi \sigma_c^2}{36\xi^3 \chi^5 (1+f)^5 (1-f)} \{a^6 \xi^3 + 8b^2 \xi^3 (R^2 + \xi^2)^2 + 2a^4 \xi [19b^4 - 5R^2 z^2 + 3z^4 + 2b^2 (5R^2 + 11z^2)] + a^5 [10b^4 + 4z^4 + b^2 (3R^2 + 14z^2)] + 2ab^2 [19b^6 + 3R^6 + 21R^4 z^2 + 37R^2 z^4 + 19z^6 + b^4 (37R^2 + 57z^2) + b^2 (21R^4 + 74R^2 z^2 + 57z^4)] + a^2 \xi [73b^6 + 3b^4 (38R^2 + 49z^2) + z^2 (R^4 - 10R^2 z^2 + z^4) + b^2 (43R^4 + 104R^2 z^2 + 75z^4)] + a^3 [72b^6 + 4z^4 (-5R^2 + z^2) + b^4 (73R^2 + 148z^2) + b^2 (9R^4 + 53R^2 z^2 + 80z^4)]\}, \quad (22)$$

$$T_z^z = -\frac{\pi a^4 G \sigma_c^2}{18\xi^2 \chi^5 (1+f)^5 (1-f)} \{-a^6 \xi^2 - 4a^5 \xi^3 - 2a^4 \xi^2 (b^2 - 2R^2 + 3z^2) + 4a^3 \xi [3b^4 + b^2 (5R^2 + 2z^2) + 2R^2 z^2 - z^4] + a^2 [23b^6 + 9b^4 (4R^2 + 5z^2) + b^2 (8R^4 + 40R^2 z^2 + 21z^4) - z^2 (R^4 - 4R^2 z^2 + z^4)] + 4ab^2 \xi [4b^4 + b^2 (7R^2 + 8z^2) + 3R^4 + 7R^2 z^2 + 4z^4] + 4b^2 \xi^2 (R^2 + \xi^2)^2\}, \quad (23)$$

$$T_\varphi^\varphi = -\frac{a^4 G \pi \sigma_c^2}{36\xi^3 \chi^5 (1+f)^5 (1-f)} \{a^6 \xi^3 + 8b^2 \xi^3 (R^2 + \xi^2)^2 + 2a^4 \xi [19b^4 + z^2 (R^2 + 3z^2) + 2b^2 (8R^2 + 11z^2)] + a^5 [10b^4 + 4z^4 + b^2 (3R^2 + 14z^2)] + 2ab^2 [19b^6 + 3R^6 + 21R^4 z^2 + 37R^2 z^4 + 19z^6 + b^4 (37R^2 + 57z^2) + b^2 (21R^4 + 74R^2 z^2 + 57z^4)] + a^2 \xi [73b^6 + z^2 (R^2 + z^2)^2 + 21b^4 (6R^2 + 7z^2) + b^2 (43R^4 + 128R^2 z^2 + 75z^4)] + a^3 [72b^6 + 4z^4 (R^2 + z^2) + b^4 (97R^2 + 148z^2) + b^2 (9R^4 + 101R^2 z^2 + 80z^4)]\}, \quad (24)$$

$$T_z^R = T_R^z = \frac{a^6 G \pi R z \sigma_c^2}{6\xi \chi^5 (1+f)^5 (1-f)} [a^3 - R^2 (a + \xi) + \xi (3a^2 + \xi^2 + 3a\xi)]. \quad (25)$$

In this case the tangential velocity and the angular momentum for a particle in circular orbits are

$$v_c^2 = \frac{2\pi G \sigma_c a^2 c^2 R^2 (2R^2 + 2\xi^2 + a\xi - a^2)}{(1-f)[3c^2 \chi^{5/2} (1+f) - 2\pi G \sigma_c a^2 R^2 (2R^2 + 2\xi^2 + a\xi - a^2)]}, \quad (26)$$

$$h = cR^2 (1+f)^2 \times \sqrt{\frac{2\pi G a^2 \sigma_c (2R^2 + 2\xi^2 + a\xi - a^2)}{3c^2 \chi^{5/2} (1-f^2) - 2\pi G \sigma_c a^2 R^2 (2R^2 + 2\xi^2 + a\xi - a^2) (2-f)}}. \quad (27)$$

where the values of ξ and χ have to be evaluated in the plane $z = 0$.

In Fig. 1 we present the surface and level curves of the energy density and the stresses for the parameters $a = 1$, $b = 0.5$ and $\sigma_c = 0.1$. Hereafter we used $G = c = 1$ for the plots and numerical calculations. As in the Newtonian case, the lower the ratio b/a the flatter the mass distribution. Numerically we verified, that

for these values $\rho > 0$ and $\epsilon > 0$, moreover $|p_+/\rho| < 0.017$, $|p_-/\rho| < 0.051$ and $|p_\varphi/\rho| < 0.051$, which means that the strong, weak and dominant energy conditions are satisfied. From the energy density profile and level curves we see that we have a ring structure. In Fig. 2 we show the tangential velocity and the angular momentum for a particle in circular orbit for the same values of Fig. 1 and different values of the parameter b . Applying the criterion of stability (18) we see that these orbits are stable. For lower values of the parameter b , e.g. $b = 0.4$, the stresses become negative, first near $R \approx 0$ and $z \approx 0$ and latter spreading to nearest values of R and z . This negatives values characterized tensions instead of pressures. The stability criterion indicates that, in this cases, the orbits in the plane $z = 0$ are non-stable in the region where we have tensions.

3.2. Disc with a ring

Following the previous section, we start with the Newtonian potential that represent a disc with a flat ring, say

$$\begin{aligned} \phi = & -\frac{2\pi\sigma_c G a^2}{15[R^2 + (a + |z|)^2]^{5/2}} \{ [R^2 + (a + |z|)^2]^2 (3 - 4k^2) + [R^2 + (a + |z|)^2] \\ & \times [a(a + |z|)(3 - 4k^2) + k^4(8R^2 + 8|z|^2 + 9a|z|)] + a^2[-R^2(1 + 2k^2) + (a + |z|)^2 \\ & \times (2 + 4k^2 + 3k^4)] \}, \end{aligned} \quad (28)$$

where k is a constant related to the disk radius. This potential corresponds to the $\phi_{(d)}^{(2)}$ potential of ¹¹. To generate the three dimensional ring model we perform the transformation $|z| \rightarrow \sqrt{z^2 + b^2}$ and we obtain

$$\begin{aligned} \Phi = & -\frac{2\pi\sigma_c G a^2}{15\chi^{5/2}} \{ \chi^2(3 - 4k^2) + \chi[a(a + \xi)(3 - 4k^2) + k^4(8R^2 + 8\xi^2 + 9a\xi)] \\ & + a^2[-R^2(1 + 2k^2) + (a + \xi)^2(2 + 4k^2 + 3k^4)] \} \end{aligned} \quad (29)$$

where ξ and χ are defined as in the previous section. The energy density and the stresses are obtained from equations (2)-(6) and relation (7). Then, the tangential velocity and the angular momentum of a circular orbital in the plane of the discs are found from (16) and (17). The analytical expressions for all these quantities are cumbersome and will be omitted. In Fig. 3 we plot the surface and level curves of the energy density and the stresses for the model of equation (29) with parameter values $a = k = 1$, $b = 0.5$ and $\sigma_c = 0.1$. Numerically we found that $\rho > 0$, $\epsilon > 0$, $|p_+/\rho| < 0.024$, $|p_-/\rho| < 0.043$ and $|p_\varphi/\rho| < 0.028$, and therefore all the energy conditions are met. In the energy density graph, the figure is plot in such a way to enhance the region in which we clearly see the ring peak and not the disc central peak. For lower values of the parameter b the disc and the ring became narrower. Note that in the p_+ graph, the stress is negative in the intersection between the disc and the ring representing tensions and not pressures. The other stresses, p_- and p_φ , are always positive. In Fig. 4, we plot the tangential velocity and the angular momentum for a circular orbiting particle for the same parameter values of Fig. 3

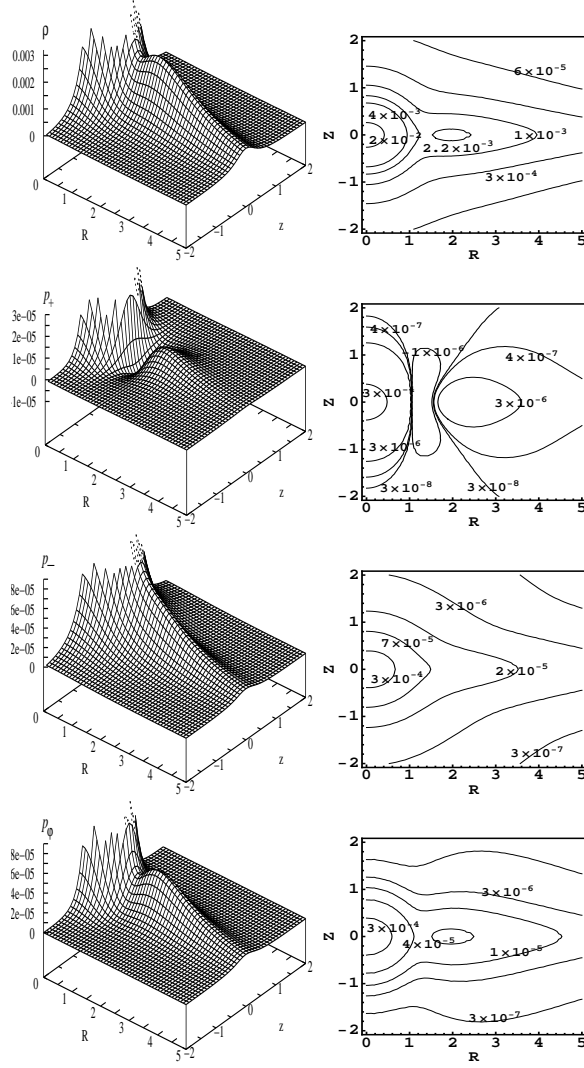


Fig. 3. Surface plots and level curves for the energy density and the stresses for the general relativistic case of a disc with a ring. The parameter values are $a = k = 1$, $b = 0.5$ and $\sigma = 0.1$. The graphs are plotted in such a way to enhance the ring peak and not the central disc peak. Note that the stress p_+ has negative values in the intersection of the disc and the ring.

and different values of the parameter b . Using the stability criterion (18), we see that for $b = 0.1$ the particle orbit is not stable for radius between $R \approx 1$ and $R \approx 1.5$. For higher values of b the circular orbits are stable. We check also that for lower values of b (thinner systems) regions of non-stability appear. This non-stability corresponds to the valley in the tangential velocity graph, and also to the radius where the stress p_+ has negative values. Moreover, we find that for lower values of the parameter b the negative value region in the stress p_+ becomes larger.

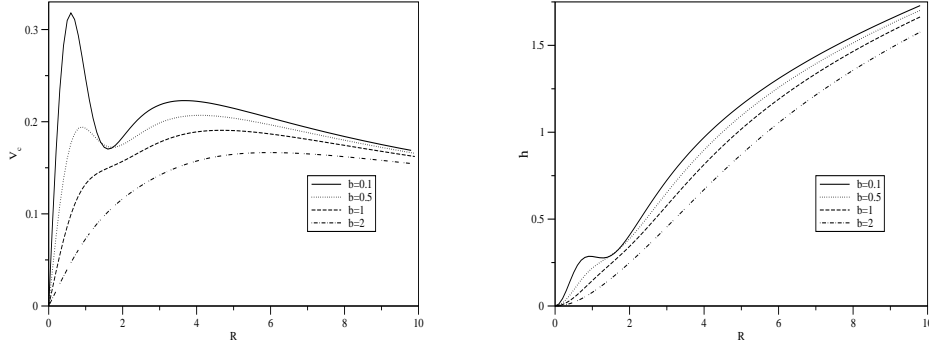


Fig. 4. Tangential velocity and angular momentum for a particle orbiting the $z = 0$ plane for the same parameter values of Fig. 3 and $b=0.1, 0.5, 1, 2$. The angular momentum curve with $b = 0.1$ has a region of non-stability near the radius 1.5 that corresponds to the valley at the same radius in the tangential velocity graph.

3.3. Double ring system

In this case, the Newtonian potential to be consider is the first member of the family of double rings find in Ref. 11, which is

$$\begin{aligned} \phi = & \frac{-2\pi\sigma_c G a^2}{105[R^2 + (a + |z|)^2]^{7/2}} \{6[R^2 + (a + |z|)^2]^3(1 + 8k^4) + [R^2 + (a + |z|)^2]^2 \\ & \times [-16k^2(R^2 + |z|^2) + a^2(9 - 26k^2 - 54k^4) + 3a|z|(2 - 16k^2 - 19k^4)] - a^2[R^2 \\ & + (a + |z|)^2][2R^2(2 + 11k^2 + 9k^4) + |z|^2(1 - 26k^2 - 27k^4) - a|z|(13 + 82k^2 \\ & + 69k^4) - 2a^2(7 + 28k^2 + 21k^4)] - 3a^3(a + |z|)(1 + k^2)^2[2R^2 + 7(a + |z|)^2]\}, \end{aligned} \quad (30)$$

where k is a constant related to the location of the gap between the rings. This potential corresponds to the $\phi_{(d)}^{(2)}$ potential of Ref. 11. Performing the previously applied transformation $|z| \rightarrow \sqrt{z^2 + b^2}$ we obtain

$$\begin{aligned} \Phi = & \frac{-2\pi\sigma_c G a^2}{105\chi^{7/2}} \{6\chi^3(1 + 8k^4) + \chi^2[-16k^2(R^2 + \xi^2) + a^2(9 - 26k^2 - 54k^4) \\ & + 3a\xi(2 - 16k^2 - 19k^4)] - a^2\chi[2R^2(2 + 11k^2 + 9k^4) + \xi^2(1 - 26k^2 - 27k^4) \\ & - a\xi(13 + 82k^2 + 69k^4) - 2a^2(7 + 28k^2 + 21k^4)] - 3a^3(a + \xi)(1 + k^2)^2 \\ & \times [2R^2 + 7(a + \xi)^2]\}, \end{aligned} \quad (31)$$

where ξ and χ are defined as in the previous section. The exact expressions for the energy density, the stresses, the tangential velocity and the angular momentum, are obtained straightforward from equations (2)-(6), (16) and (17) using (7). In Fig. 5, we plot the surface and level curves of the energy density and the stresses for the double ring system for parameter values $a = k = 1$, $b = 0.5$ and $\sigma_c = 0.1$. For this parameter values we found that $\rho > 0$, $\epsilon > 0$, $|p_+/\rho| < 0.028$, $|p_-/\rho| < 0.023$

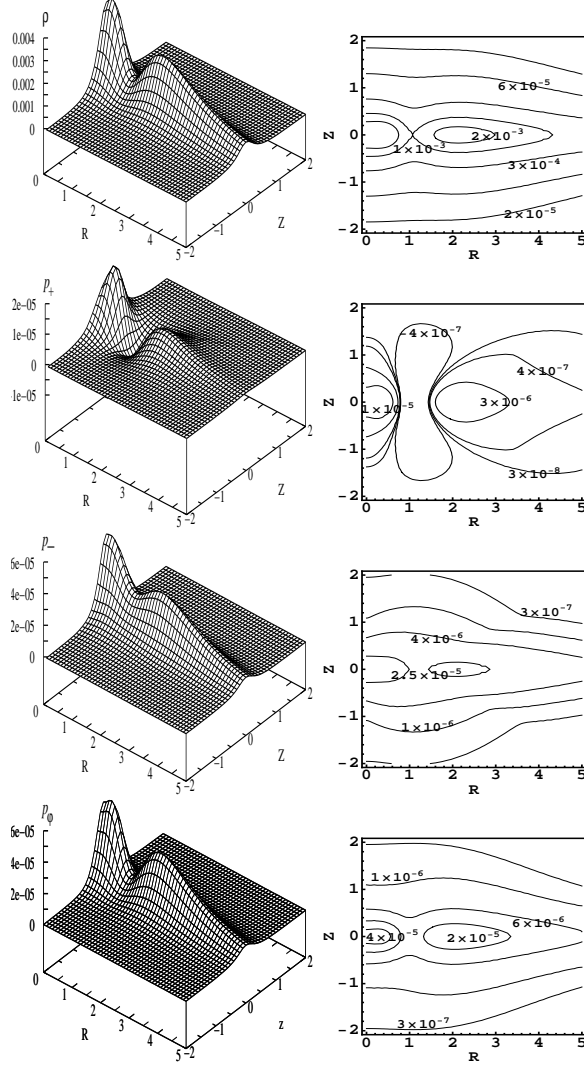


Fig. 5. Surface plots and level curves for the energy density and the stresses for the general relativistic case of a two ring system. The parameter values are $a = k = 1$, $b = 0.5$ and $\sigma = 0.1$. Note that the stress p_+ has negative values in the intersection of the rings.

and $|p_\phi/\rho| < 0.023$, and the model satisfies all the energy conditions. The energy density graph shows two ring peaks of approximately the same magnitude. The p_+ stress has negative values between the rings, this is similar to what we find in the disc with a ring case. The other stresses are positive. As in the Newtonian case, for lower values of the ratio b/a the two rings became thinner. In Fig. 6, we plot the tangential velocity and the angular momentum of the particle with the same parameter values of Fig. 5 and different values of the parameter b . We see from the

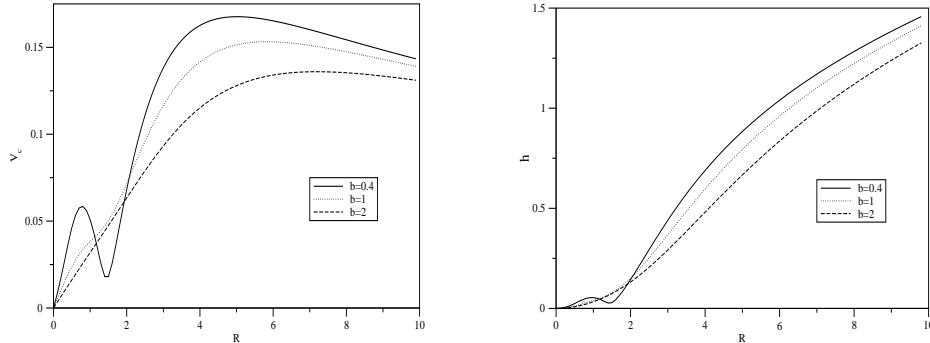


Fig. 6. Tangential velocity and angular momentum for a particle orbiting the $z = 0$ plane for the same parameter values of Fig. 5 and $b=0.4, 1, 2$. The angular momentum curve with $b = 0.4$ has a region of non-stability from $R \approx 1$ to $R \approx 1.5$.

angular momentum graph, that for $b = 0.4$ the circular orbits are non-stable in a region between $R \approx 1$ and $R \approx 1.5$. Note that this correspond, as in the disc with a ring case, to the valley located at the same radius in the tangential velocity profile for the same value of b . But, the tangential velocity curves are a bit different from the disc and a ring case because the starting values of the monotonically decreasing region ($R > 4$ approximately) are higher than the initial bump. For higher values of the parameter b the circular orbits are always stable. Also, we find that when we lower the parameter b , the negative value region in the stresses increases.

4. Conclusions

In this work we presented several ring model systems in the context of general relativity. This was achieved by inflating previously constructed Newtonian ring potentials using the transformation $|z| \rightarrow \sqrt{z^2 + b^2}$, and then finding their relativistic analogs. We use an inverse method because, in general, the direct method for solving Einstein's field equations for more sophisticated models is difficult and cumbersome, and in most of the cases the solutions do not have a clear physical interpretation at the newtonian limit, making these solutions, in some sense, useless. In the other hand, if we want to solve the Einstein field equations using the direct method for a more sophisticated model, say several concentric rings of matter, we do not know how to construct the correct form of the energy momentum tensor of our system, and maybe after solving it we do not have a clear physical interpretation at the newtonian limit.

The models presented in this work have infinite extension but the physical quantities decays very fast with the distance, and in principle, one could make a cut-off radius to consider it finite. The different systems studied present a region of non-stability in the intersection of the disc and the ring, and between the rings. This region of non-stability is present in thinner systems and corresponds to a region in

which one of the stresses is negative, i.e. we have tensions instead of pressures. A better approach to the stability of the system has to take into account the collective behavior of the particles and not only a geodesic approximation. This will be done in a future work. Some examples of general relativistic stability analysis of discs can be found in Ref. 24, 25, 26.

In summary, this article shows several general relativistic ring systems that are physical acceptable and have a clear interpretation at the newtonian limit, and from which we can test general relativistic effects.

Acknowledgements

M.U. and P.S.L. thanks CNPq for financial support; P.S.L. also thanks FAPESP; D.V. thanks FAPESP for financial support.

References

1. J. C. Theys and E. A. Spiegel, *Astrophys. J.* **208** (1976) 650.
2. J. C. Theys and E. A. Spiegel, *Astrophys. J.* **212** (1977) 616.
3. B. C. Whitmore *et al.*, *Astron. J.* **100** (1990) 1489.
4. P. Appell, *Ann. Math., Lpz.* **30** (1887) 155.
5. E. T. Whittaker and G. N. Watson, *A Course of Modern Analysis* (Cambridge University Press, Cambridge, 1950).
6. R. Gleiser and J. Pullin, *Class. Quantum Grav.* **6** (1989) 977.
7. P. S. Letelier and S. R. Oliveira, *J. Math. Phys.* **28** (1987) 16.
8. Lord Kelvin, *J. Math. Pures Appl.* **12** (1847) 256.
9. T. Morgan and L. Morgan, *Phys. Rev.* **183** (1969) 1097.
10. P. S. Letelier, *Mon. Not. R. Astron. Soc.* **381** (2007) 1031.
11. D. Vogt and P. S. Letelier, *Mon. Not. R. Astron. Soc.* **396** (2009) 1487.
12. G. G. Kuzmin, *Astron. Zh.* **33** (1956) 27.
13. A. Toomre, *Astrophys. J.* **138** (1963) 385.
14. L. Ciotti and G. Giampieri, *Mon. Not. R. Astron. Soc.* **376** (2007) 1162.
15. L. Ciotti and F. Marinacci, *Mon. Not. R. Astron. Soc.* **387** (2008) 1117.
16. S. K. Chakrabarti, *Astron. Astrophys.* **9** (1988) 49.
17. J. P. S. Lemos and P. S. Letelier, *Phys. Rev. D* **49** (1994) 5135.
18. O. Semerák, M. Žáček and T. Zellerin, *Mon. Not. R. Astron. Soc.* **308** (1999) 705.
19. O. Semerák, T. Zellerin and M. Žáček, *Mon. Not. R. Astron. Soc.* **308** (1999) 691.
20. D. Vogt and P. S. Letelier, *Mon. Not. R. Astron. Soc.* **363** (2005) 268.
21. P. S. Letelier, *Phys. Rev. D* **68** (2003) 104002.
22. Lord Rayleigh, *Proc. R. Soc. London A* **93** (1916) 148.
23. L. D. Landau and E. M. Lifshitz, *Fluid Mechanics* (Butterworth-Heinemann, Oxford, 1987).
24. M. Ujevic and P. S. Letelier, *Phys. Rev. D* **70** (2004) 084015.
25. M. Ujevic and P. S. Letelier, *Gen. Relativ. Gravit.* **39** (2007) 1345.
26. M. Ujevic and P. S. Letelier, *Mon. Not. R. Astron. Soc.* **381** (2007) 1499.
27. D. Vogt and P. S. Letelier, *Phys. Rev. D* **68** (2003) 084010.
28. M. Miyamoto and R. Nagai, *Publ. Astron. Soc. Jpn.* **27** (1975) 533.